



Estimating the contribution of ion–ion recombination to sub-2 nm cluster concentrations from atmospheric measurements

J. Kontkanen¹, K. E. J. Lehtinen², T. Nieminen^{1,3}, H. E. Manninen¹, K. Lehtipalo^{1,4}, V.-M. Kerminen¹, and M. Kulmala¹

¹Department of Physics, University of Helsinki, Helsinki, Finland

²Department of Applied Physics, University of Eastern Finland and Finnish Meteorological Institute, Kuopio, Finland

³Helsinki Institute of Physics, Helsinki, Finland

⁴Airmodus Oy, Helsinki, Finland

Correspondence to: J. Kontkanen (jenni.kontkanen@helsinki.fi)

Received: 5 July 2013 – Published in Atmos. Chem. Phys. Discuss.: 9 August 2013

Revised: 16 October 2013 – Accepted: 24 October 2013 – Published: 25 November 2013

Abstract. The significance of ion–ion recombination for atmospheric new particle formation is not well quantified. Here we present and evaluate a method for determining the size distribution of recombination products from the size distributions of neutral and charged clusters. Our method takes into account the production of recombination products in the collisions between oppositely charged ions and the loss due to coagulation. Furthermore, unlike previous studies, we also consider the effect of condensational growth on the size distribution of recombination products. We applied our method to the data measured in Hyytiälä, Finland, to estimate the contribution of ion–ion recombination to the concentrations of atmospheric clusters in the size range of 0.9–2.1 nm. We observed that the concentration of recombination products was highest in the size classes between 1.5 and 1.9 nm. The median concentrations of recombination products were between 6 and 69 cm⁻³ in different size classes, which resulted in a small proportion of all neutral clusters, varying between 0.2 and 13 %. When examining the whole size range between 0.9 and 2.1 nm, the median fraction of recombination products of all neutral clusters was only 1.5 %. We also investigated how the results change if the effect of condensational growth is neglected. It seems that with that assumption the fragmentation of newly formed recombination products has to be taken into account, or else the concentration of recombination products is overestimated. Overall, we concluded that our method provides reasonable results, which are consistent with the earlier estimates on the contribution of recombination products to atmospheric cluster population in

Hyytiälä. Still, in order to determine the size distribution of recombination products more accurately in the future, more precise measurements of the size distribution of atmospheric clusters would be needed.

1 Introduction

New particle formation is, in terms of the particle number concentration, the dominant source of aerosol particles in the atmosphere (Spracklen et al., 2006; Yu et al., 2010). The process may also influence the Earth's climate via the indirect climate effects of aerosol particles (Merikanto et al., 2009; Wang and Penner, 2009; Kazil et al., 2010; Kerminen et al., 2012; Makkonen et al., 2012). New particle formation includes the production of nanometer-sized clusters from atmospheric vapors and the growth of the clusters to larger particles. Although recent studies have provided new insight into the first steps of new particle formation, the picture is still not complete (Zhang et al., 2012; Kulmala et al., 2013). To understand the details of new particle formation better, more knowledge of the dynamics of neutral and charged clusters in the atmosphere is needed.

One dynamic process modifying the size distributions of neutral and charged clusters is ion–ion recombination. In ion–ion recombination two oppositely charged ions collide and form a neutral cluster. The role of ion–ion recombination as a sink for air ions has been known for decades, and the rate of the process and its dependency on environmental

conditions has been widely studied (e.g. Nolan, 1941; McGowan, 1965; Biondi, 1968; Bates, 1985; Hoppel and Frick, 1986; Sorokin and Mirabel, 2001; Tammet et al., 2006). More recently, researchers have also attempted to estimate the importance of ion–ion recombination for atmospheric new particle formation (e.g. Turco et al., 1998). Kulmala et al. (2007) introduced a method to determine the concentration of recombination products from ion size distribution measurements. They concluded that ion–ion recombination has only a minor contribution to particle formation in boreal forest conditions. Subsequently, other studies using the same approach have obtained similar results (Manninen et al., 2009a; Lehtipalo et al., 2009). Kulmala et al. (2013) were the first to determine the concentration of recombination products in different size classes in the sub-2 nm size range. Thus, they were able to show that in all those size classes the proportion of recombination products of all clusters is small in boreal forest. However, the model studies by Yu and Turco (2008) suggest that ion–ion recombination is much more significant than indicated by the measurements.

Although the importance of recombination has been estimated from measurements in several studies, the applied methods have not been properly evaluated. In addition, the effect of condensational growth on the size distribution of recombination products has not been included in the calculations. Hence, in this paper, we present and evaluate a method to determine the size distribution of recombination products from measurements by considering the production of recombination products in the collisions between oppositely charged ions, the loss by coagulation and the loss and gain due to condensational growth. First, we derive the equation for the concentration of recombination products in a certain size range. Then, we show how the production and loss rates of recombination products can be calculated from the measured data. We also apply our method to the data measured in Hyytiälä, Finland, to assess the role of ion–ion recombination in the dynamics of sub-2 nm neutral and charged clusters. Finally, we examine the sensitivity of our method to uncertainties related to the effect of condensational growth.

2 Methods

2.1 Measurements

The measurements were carried out between 14 March and 10 May 2011 at the SMEAR II station (Station for Measuring Forest Ecosystem-Atmosphere Relations) in Hyytiälä, southern Finland (61°51' N, 24°17' E; 181 m above sea level) (Hari and Kulmala, 2005). The total concentration of neutral and charged clusters in six equally spaced size classes ranging from 0.9 to 2.1 nm in mobility diameter was measured with the Airmodus A09 particle size magnifier (PSM; Vanhanen et al., 2011). The ion concentrations in the same size classes were measured with the Neutral cluster and Air

Ion Spectrometer (NAIS; Manninen et al., 2009b; Mirme and Mirme, 2013). By subtracting ion concentration from the total concentration, we also obtained the concentration of neutral clusters in different size classes. Due to the measurement uncertainties of both PSM and NAIS, the lowest reliable values of neutral cluster concentration were estimated to be 100–200 cm⁻³. In addition to PSM and NAIS data, we used particle size distributions continuously measured at the station between 3 and 1000 nm with the twin-DMPS (differential mobility particle sizer) system (Aalto et al., 2001). For the more detailed description of the performed measurements, see Kulmala et al. (2013).

2.2 Determining the size distribution of recombination products

2.2.1 Equation for the concentration of recombination products

Here we derive an expression for the concentration of neutral clusters due to ion–ion recombination, N_{rec} . The time evolution of the concentration of recombination products in a certain size range i can be described by the balance equation

$$\begin{aligned} \frac{dN_{\text{rec},i}}{dt} = & \lambda_i \alpha \sum_{j,k} r_{ijk} N_j^+ N_k^- - 2\beta N_{\text{rec},i} \sum_j N_j^\pm \\ & - \text{CoagS}_i N_{\text{rec},i} + \frac{N_{\text{rec},i-1}}{\Delta D_p} \text{GR}_{i-1} - \frac{N_{\text{rec},i}}{\Delta D_p} \text{GR}_i + Q_i. \end{aligned} \quad (1)$$

Here α is the ion–ion recombination coefficient and β the ion-neutral attachment coefficient for which the values of $1.6 \times 10^{-6} \text{ cm}^3 \text{ s}^{-1}$ and $0.01 \times 10^{-6} \text{ cm}^3 \text{ s}^{-1}$ are used (Hoppel and Frick, 1986; Tammet and Kulmala, 2005). However, it has to be noted that, in reality, these coefficients may not be constant but depend on the properties of colliding ions or particles and environmental conditions (Bates, 1985; Hoppel and Frick, 1986). The coefficient λ_i describes the fraction of stable recombination products that does not fragment instantly after their formation in size class i . N_j^+ and N_k^- refer to the concentrations of the positive and negative ions in size ranges j and k , respectively, and r_{ijk} tells how large fraction of the recombination products formed in their collisions will end up in size class i . CoagS_i denotes the average coagulation sink for size range i . GR_{i-1} and GR_i refer to the growth rates of clusters in size ranges $i-1$ and i due to condensation, and ΔD_p is the width of the size range. Finally, Q_i denotes the source of clusters to size class i originating from the break-ups of larger clusters formed by recombination. Note that the summations in the first two terms on the right-hand side go through the ion size classes.

Accordingly, Eq. (1) includes the terms for the production of neutral clusters in the collisions between two oppositely charged ions (the first term), the loss of neutral clusters due to charging (the second term), the loss by coagulation (the third term), and the gain and loss of neutral clusters due to the condensational growth of clusters into the size class and out

of the size class (the fourth and the fifth terms). In addition, the last term allows for the possibility that breaking up of larger recombination products may produce clusters into size range i .

In order to estimate the concentration of recombination products from Eq. (1), we first simplify the equation by neglecting the last term describing the production of clusters due to breaking up of larger clusters. This simplification may cause errors in the smallest size classes, but the effect on the final results is likely to be only minor. Now, by defining the plain production rate of neutral clusters by recombination as

$$R_{r,i} = \alpha \sum_{j,k} r_{ijk} N_j^+ N_k^-, \quad (2)$$

we may write Eq. (1) as

$$\frac{dN_{rec,i}}{dt} = \lambda_i R_{r,i} - 2\beta N_{rec,i} \sum_j N_j^\pm - \text{CoagS}_i N_{rec,i} - \frac{\text{GR}_i}{\Delta D_p} \left(1 - \frac{\text{GR}_{i-1}}{\text{GR}_i} \frac{N_{rec,i-1}}{N_{rec,i}} \right) N_{rec,i}. \quad (3)$$

In pseudo-steady state, Eq. (3) becomes

$$N_{rec,i} = \frac{\lambda_i R_{r,i}}{\text{CoagS}_i + 2\beta \sum_j N_j^\pm + \frac{\text{GR}_i}{\Delta D_p} \left(1 - \frac{\text{GR}_{i-1}}{\text{GR}_i} \frac{N_{rec,i-1}}{N_{rec,i}} \right)}. \quad (4)$$

Now, let us examine the magnitudes of different terms in the denominator of Eq. (4). From the particle size distributions measured during spring 2011 in Hyytiälä, we obtain that the average coagulation sink for the clusters in the size range of 1–2 nm (CoagS) was 10^{-3} s^{-1} . From the NAIS data measured at the same time, we get the average ion concentration, $\sum_j N_j^\pm$, of 800 cm^{-3} and consequently the term describing the loss of neutral clusters due to charging ($2\beta \sum_j N_j^\pm$) is equal to $1.6 \times 10^{-5} \text{ s}^{-1}$. Thus, we may notice that $\text{CoagS}_i \gg 2\beta \sum_j N_j^\pm$, and Eq. (4) can be written as

$$N_{rec,i} = \frac{\lambda_i R_{r,i}}{\text{CoagS}_i + \frac{\text{GR}_i}{\Delta D_p} \left(1 - \frac{\text{GR}_{i-1}}{\text{GR}_i} \frac{N_{rec,i-1}}{N_{rec,i}} \right)}. \quad (5)$$

By considering typical air ion concentrations in the atmosphere (Hirsikko et al., 2011), and estimating the variation of coagulation sink based on the reported aerosol number size distributions (Raes et al., 2000), we may conclude that Eq. (5) should be generally valid in the lower troposphere.

From Eq. (5) we can see that the effect of condensational growth on the recombination product concentration depends on the rates at which the concentration of recombination products and cluster growth rate change with the increasing cluster size. However, by assuming that the condensational flux of recombination products to the smallest size class is negligible, we end up with a recursive algorithm that allows for the solution of $N_{rec,i}$ in an analytical form. This requires,

however, that we know the cluster growth rate both in size class i and in the size class preceding it, which is rarely the case. Thus, we can either assume certain growth rates for the examined size classes and calculate the concentration of recombination products from Eq. (5), or then we can assume that the effect of condensational growth on the recombination product concentration is negligible compared with coagulation sink. With the latter assumption the equation for the concentration of recombination products in size class i is reduced to the form

$$N_{rec,i} = \frac{\lambda_i R_{r,i}}{\text{CoagS}_i}. \quad (6)$$

In previous studies (e.g. Kulmala et al., 2013) Eq. (6) has been used to calculate the concentration of recombination products. In this study we first present the results obtained when calculating the concentration of recombination products in different size classes between 0.9 and 2.1 nm from Eq. (5), which includes the condensational growth term. After that we examine closer how the changes in the growth rates, or neglecting the condensational growth term and using Eq. (6), affect the results.

2.2.2 Calculating the production and loss rates of recombination products

According to Eq. (5), the concentration of recombination products in a certain size range is determined by the production of them in the collisions between oppositely charged ions (the term in the numerator), the loss by coagulation (the first term in the denominator) and the gain and loss due to the condensational growth into the size range and out of the size range (the second term in the denominator). The loss due to coagulation, described by the coagulation sink (CoagS_{*i*}), we can calculate from particle size distributions (Kulmala et al., 2001). The estimates for growth rates (GR_{*i*}), needed for the condensational growth term, we can obtain from cluster diameter vs. time data presented by Kulmala et al. (2013). The values for growth rates in each size class can be obtained by fitting the data with a third-degree polynomial and differentiating (Table 1). However, to calculate the production rate of recombination products, we need to know both the value of the coefficient λ_i , representing the fraction of stable recombination products, and the plain production rate of neutral clusters by recombination, $R_{r,i}$.

Let us first determine the plain production rate of neutral clusters by recombination, $R_{r,i}$. From Eq. (2) we can see that $R_{r,i}$ in size class i depends on the concentrations of positive and negative ions, N_j^+ and N_k^- , that form a neutral cluster to that size class when colliding with each other. We can get N_j^+ and N_k^- from the ion mobility distributions measured with an ion spectrometer, a NAIS in our case. The NAIS measures the mobility distribution of ions over 28 mobility bins ranging from 3.2 to $0.0013 \text{ cm}^2 \text{ V}^{-1} \text{ s}^{-1}$ (Manninen et al., 2009b; Mirme and Mirme, 2013). We can convert these

Table 1. Growth rates for different size classes between 0.9 and 2.1 nm. GR_{fit} shows the growth rates obtained by fitting a third-degree polynomial to experimental data, and differentiating. GR_{low} shows the growth rates used for analyzing the sensitivity of the results to the changes in the growth rates.

Size range [nm]	GR_{fit} [nm h ⁻¹]	GR_{low} [nm h ⁻¹]
0.9–1.1	0.2	0.2
1.1–1.3	0.5	0.3
1.3–1.5	0.7	0.4
1.5–1.7	1.0	0.5
1.7–1.9	1.2	0.6
1.9–2.1	1.4	0.7

mobility bins to mass bins by using a relationship between ion mobility and mass presented by Mäkelä et al. (1996):

$$Z = \exp\left(-0.0347(\ln(m))^2 - 0.0376\ln(m) + 1.4662\right). \quad (7)$$

Here Z is the electrical mobility in $\text{cm}^2 \text{V}^{-1} \text{s}^{-1}$ and m the ion mass in amu. Equation (7) is based on the data by Kilpatrick et al. (1971) for ions in nitrogen. The data have been commonly used in conversions between mobility and mass, although the applicability of the data under atmospheric conditions has been questioned (e.g. Böhringer et al., 1987; Tammet, 1995). In addition, the relationship between ion mobility and mass may in reality depend on the polarity (Swider, 1988). For the comparison of the relationship between mass, mobility and diameter determined by using different methods, see Ehn et al. (2011).

The mass ranges corresponding to the mobility ranges of different NAIS channels according to Eq. (7) are presented in Table 2. From the mass ranges of different channels we can determine the lower and upper limits for the masses of recombination products formed in the collisions between ions from different channels. This can be done for each pair of recombining ions by adding up their smallest possible masses and their largest possible masses. The mass limits of the recombination products can then be converted to mobilities by using Eq. (7). Thereafter, we may convert the mobilities into mobility diameters using the modified Stokes–Millikan equation, which takes into account the finite mass of the particle (Tammet, 1995; Ehn et al., 2011):

$$d_p = \frac{1}{\sqrt{1 + m_g/m}} \frac{qC_c(d_p)}{3\pi\mu Z}. \quad (8)$$

Here d_p denotes the mobility diameter, m_g the mass of an air molecule and m the mass of the particle. q is the number of electrical charges in the particle, μ is the dynamic viscosity of air and Z the electric mobility of the particle. C_c is the slip correction factor taking into account non-continuum effects, which become important at small sizes. Note that in earlier studies (e.g. Kulmala et al., 2013) mobilities have

been converted to diameters according to the original form of Stokes–Millikan equation, which does not include the mass-dependent factor on the right-hand side of Eq. (8).

Table 3 shows the mass and diameter limits of the recombination products for the pairs of recombining ions from different NAIS channels. From the diameter limits we are able to resolve the contribution of different ion pairs $N_j^+ N_k^-$ to the production rate of neutral clusters by recombination in size class i .

This we can do by determining for each pair of ions the factor r_{ijk} , which describes how large fraction of the recombination products of that ion pair will end up in size class i . The value for the factor r_{ijk} can be resolved for each ion pair $N_j^+ N_k^-$ by calculating how large fraction of the size range of their recombination products overlaps with size class i . Finally, we can calculate the plain production rate of neutral clusters by recombination, $R_{r,i}$, for each size class from Eq. (2).

After calculating the plain production rate, $R_{r,i}$, for each size class, we can estimate the maximum fraction of stable recombination products, $\lambda_{\text{max},i}$, from the measured size distributions of neutral and charged clusters by using the method presented by Kulmala et al. (2013). The first step in the analysis is to calculate the concentration of recombination products in size class i from Eq. (5) or Eq. (6) by setting the value of λ_i to unity. Furthermore, the total neutral cluster concentration in size class i can be calculated by subtracting the ion concentration, $N_{\text{ions},i}$, from the total concentration, $N_{\text{tot},i}$. After that we can estimate the maximum value of the coefficient λ_i by assuming that the concentration of recombination products cannot exceed the concentration of all neutral clusters. Thus, this method can reveal the maximum value of the coefficient λ_i only if the recombination product concentrations obtained with $\lambda = 1$ are occasionally clearly higher than the total neutral cluster concentrations. In other cases we must assume that the coefficient λ_i equals unity when estimating the maximum contribution of ion–ion recombination to cluster concentrations. The value of unity for the coefficient λ_i has also been used in several earlier studies (Kulmala et al., 2007; Lehtipalo et al., 2009; Manninen et al., 2009a).

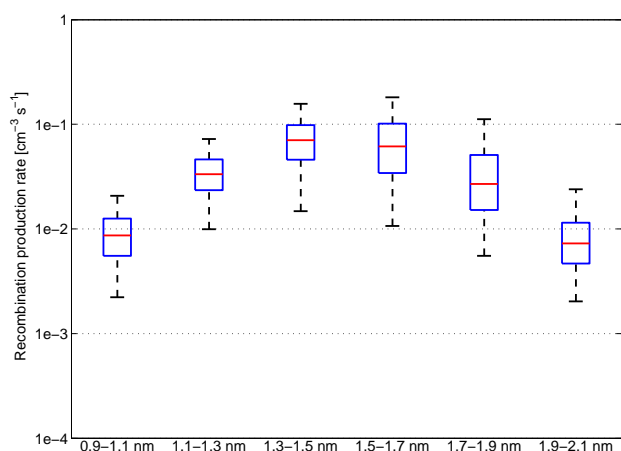
3 Results and discussion

3.1 Contribution of ion–ion recombination to cluster concentrations

By using the method described above, we calculated the plain production rate of neutral clusters by recombination, R_r , in six size classes between 0.9 and 2.1 nm (0.9–1.1 nm, 1.1–1.3 nm, 1.3–1.5 nm, 1.5–1.7 nm, 1.7–1.9 nm and 1.9–2.1 nm) (Fig. 1). The production rate had a distinct distribution with a maximum in the size classes between 1.3 and 1.7 nm in which the median production rates were $6\text{--}7 \times 10^{-2} \text{ cm}^{-3} \text{ s}^{-1}$. The lowest recombination production

Table 2. The mobility and mass ranges of the NAIS channels.

Channel	Mean mobility [cm ² V ⁻¹ s ⁻¹]	Mobility upper limit [cm ² V ⁻¹ s ⁻¹]	Mobility lower limit [cm ² V ⁻¹ s ⁻¹]	Mass lower limit [amu]	Mass upper limit [amu]
1	3.160	3.649	2.737	6	23
2	2.370	2.737	2.054	23	62
3	1.780	2.054	1.539	62	141
4	1.330	1.539	1.153	141	287
5	1.000	1.153	0.866	287	540
6	0.750	0.866	0.649	540	967
7	0.562	0.649	0.487	967	1658
8	0.422	0.487	0.365	1658	2748
9	0.316	0.365	0.274	2748	4431
10	0.237	0.274	0.205	4431	6958
11	0.178	0.205	0.154	6958	10732
12	0.133	0.154	0.115	10732	16239
13	0.100	0.115	0.087	16239	24117
14	0.075	0.087	0.065	24117	35392
15	0.056	0.065	0.049	35392	51232
16	0.042	0.049	0.037	51232	73335
17	0.032	0.037	0.027	73335	103937
18	0.024	0.027	0.021	103937	145623
19	0.018	0.021	0.015	145623	202646
20	0.013	0.015	0.012	202646	279487
21	0.010	0.012	0.009	279487	381732
22	0.008	0.009	0.006	381732	518621
23	0.006	0.006	0.005	518621	699462
24	0.004	0.005	0.004	699462	937801
25	0.003	0.004	0.003	937801	1250695
26	0.002	0.003	0.002	1250695	1656311
27	0.002	0.002	0.002	1656311	2185970
28	0.001	0.002	0.001	2185970	2877563

**Fig. 1.** The production rate of neutral clusters by recombination in different size classes. The red lines show the medians, the blue boxes indicate the 25th and 75th percentiles, and the vertical bars show the 5th and 95th percentiles.

rates were obtained in the smallest (0.9–1.1 nm) and the largest (1.9–2.1 nm) size classes in which the median values were $9 \times 10^{-3} \text{ cm}^{-3} \text{ s}^{-1}$ and $7 \times 10^{-3} \text{ cm}^{-3} \text{ s}^{-1}$, respectively. Manninen et al. (2009a) estimated that in Hyytiälä the median production rate of neutral clusters by recombination is $5 \times 10^{-2} \text{ cm}^{-3} \text{ s}^{-1}$ in the size range of 2–3 nm. However, the difference in the studied size range makes it difficult to compare our results with those of Manninen et al. (2009a).

Because the recombination production rate is solely determined by the concentrations of charged clusters, the observed size dependence of the production rate results from the ion size distribution. The ion concentration was highest between 1.1 and 1.3 nm (Table 4). The ions in this size range are measured mainly with the fourth NAIS channel. When ions from this channel collide with each other, the formed neutral clusters end up in the size classes between 1.3 and 1.7 nm, where the maximum in the recombination production rate was observed. The maximum in the ion concentration in the size class of 1.1–1.3 nm can be explained by the continuous production of small ions in the atmosphere (see Hirsikko et al., 2011, and references therein).

Table 3. The mass and size ranges of the recombination products formed in the collisions of different ion pairs. N and P refer to the negative and positive ions and the numbers from 1 to 7 to the different NAIS channels shown in Table 2.

Ion pairs	Rec. products mass lower limit [amu]	Rec. products mass upper limit [amu]	Mobility diameter lower limit [nm]	Mobility diameter upper limit [nm]
N ₁ +P ₁	12	46	0.47	0.80
N ₁ +P ₂ , N ₂ +P ₁	29	85	0.68	0.97
N ₂ +P ₂	46	124	0.80	1.09
N ₁ +P ₃ , N ₃ +P ₁	68	164	0.91	1.17
N ₃ +P ₂ , N ₂ +P ₃	85	203	0.97	1.24
N ₃ +P ₃	124	282	1.09	1.35
N ₁ +P ₄ , N ₄ +P ₁	147	310	1.14	1.39
N ₂ +P ₄ , N ₄ +P ₂	164	349	1.17	1.43
N ₃ +P ₄ , N ₄ +P ₃	203	428	1.24	1.51
N ₁ +P ₅ , N ₅ +P ₁	293	563	1.35	1.62
N ₄ +P ₄	282	574	1.37	1.63
N ₂ +P ₅ , N ₅ +P ₂	310	602	1.39	1.65
N ₃ +P ₅ , N ₅ +P ₃	349	681	1.43	1.70
N ₄ +P ₅ , N ₅ +P ₄	428	827	1.51	1.79
N ₅ +P ₅	574	1080	1.61	1.88
N ₁ +P ₆ , N ₆ +P ₁	546	990	1.62	1.90
N ₂ +P ₆ , N ₆ +P ₂	563	1029	1.63	1.93
N ₃ +P ₆ , N ₆ +P ₃	602	1108	1.65	1.94
N ₄ +P ₆ , N ₆ +P ₄	681	1254	1.70	2.01
N ₅ +P ₆ , N ₆ +P ₅	827	1507	1.79	2.12
N ₆ +P ₆	1080	1934	1.87	2.18
N ₁ +P ₇ , N ₇ +P ₁	973	1681	1.88	2.20
N ₂ +P ₇ , N ₇ +P ₂	990	1720	1.90	2.22
N ₃ +P ₇ , N ₇ +P ₃	1029	1799	1.93	2.27
N ₄ +P ₇ , N ₇ +P ₄	1108	1945	1.94	2.28
N ₅ +P ₇ , N ₇ +P ₅	1254	2198	2.01	2.36
N ₆ +P ₇ , N ₇ +P ₆	1507	2625	2.12	2.48
N ₇ +P ₇	1934	3316	2.18	2.53

Table 4. The median values for the recombination production rate (R_R) and the concentrations of recombination products (N_{rec}), all clusters (N_{tot}), charged clusters (N_{ions}) and all neutral clusters ($N_{\text{n,tot}}$) in six size classes between 0.9 and 2.1 nm.

Size range [nm]	R_R [$\text{cm}^{-3} \text{s}^{-1}$]	N_{rec} [cm^{-3}]	N_{tot} [cm^{-3}]	N_{ions} [cm^{-3}]	$N_{\text{n,tot}}$ [cm^{-3}]
0.9–1.1	9×10^{-3}	6	2955	174	2793
1.1–1.3	3×10^{-2}	24	1122	271	847
1.3–1.5	7×10^{-2}	56	873	183	653
1.5–1.7	6×10^{-2}	69	532	56	450
1.7–1.9	3×10^{-2}	69	470	16	447
1.9–2.1	7×10^{-3}	48	699	5	694

After calculating the plain production rate of neutral clusters by recombination, R_R , we calculated the concentration of recombination products in different size classes from Eq. (5) by assuming that the coefficient λ , describing the fraction of stable recombination products, equals unity in all size classes. When comparing the obtained concentrations to the concentrations of all neutral clusters following the method by Kulmala et al. (2013), we noticed that the concentrations of recombination products did not significantly exceed the con-

centrations of all neutral clusters in any of the size classes. Thus, we may assume that $\lambda = 1$ in all size classes when determining the concentration of recombination products from Eq. (5). The advantage of this assumption is that we can be sure to get the maximum estimate for the contribution of recombination to cluster concentrations. Figure 2 illustrates the obtained concentrations of recombination products in different size classes. The concentration was highest in the size classes between 1.5 and 1.9 nm in which the median

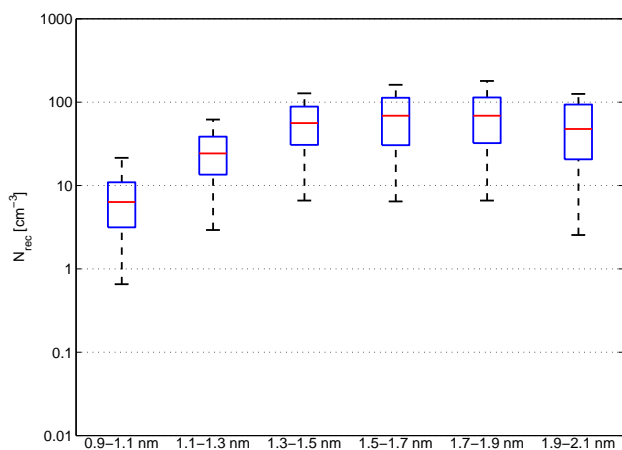


Fig. 2. The concentration of recombination products in different size classes. The red lines show the medians, the blue boxes indicate the 25th and 75th percentiles, and the vertical bars show the 5th and 95th percentiles.

concentration was 69 cm^{-3} . The lowest concentration was observed in the smallest size class (0.9–1.1 nm) with the median value of 6 cm^{-3} .

The fraction of recombination products of all neutral clusters is depicted in Fig. 3 for different size classes. The median fraction was lowest, 0.2 %, in the smallest size class (0.9–1.1 nm). The median fraction was highest, 13 %, in the size classes between 1.5 and 1.9 nm. When looking at the whole size range between 0.9 and 2.1 nm, the median fraction of recombination products of all neutral clusters was only 1.5 %. Thus, it seems that on average the contribution of ion–ion recombination to neutral cluster concentrations is low compared to other particle formation mechanisms. Furthermore, it has to be noted that in reality the proportion of recombination products of all neutral clusters is likely even smaller than obtained with our analysis, as we did not take into account the fragmentation of recombination products.

From Fig. 3 it can also be noticed that the fraction of recombination products of all neutral clusters had a strong temporal variation during the measurement period, making the ranges from 25th to 75th percentiles wide. The strong variation in the concentration of recombination products and their contribution to cluster concentrations can also be seen in Fig. 4, where the time series for the concentrations of recombination products and all neutral clusters between 0.9 and 2.1 nm are presented. In addition, Fig. 4 shows that the recombination product concentration did not have a similar diurnal cycle as the total neutral cluster concentration, which increased strongly during daytime. The reason for the difference is that the concentration of recombination products depends mainly on relatively stable ion concentrations, whereas the total neutral cluster concentration increases when there is new particle formation taking place. This can be seen in Fig. 5 as well, where the median diurnal variations of the con-

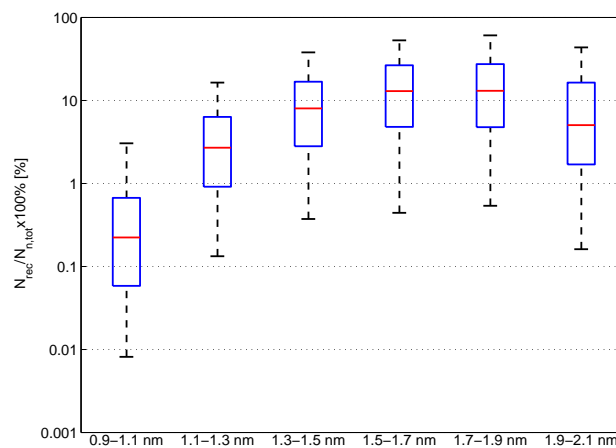


Fig. 3. The percentage of recombination products of all neutral clusters in different size classes. The red lines show the medians, the blue boxes indicate the 25th and 75th percentiles, and the vertical bars show the 5th and 95th percentiles.

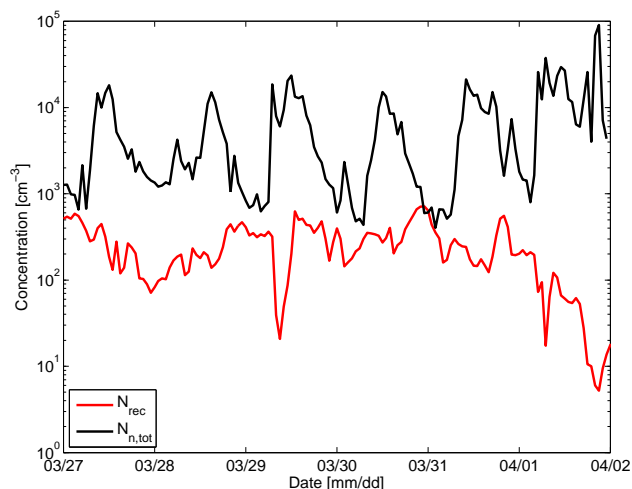


Fig. 4. The concentrations of recombination products (N_{rec}) and all neutral clusters ($N_{\text{n,tot}}$) in the size range of 0.9–2.1 nm during the period 27 March–1 April 2011. The recombination product concentration exceeded the concentration of all neutral clusters briefly on 30 March because the total neutral cluster concentration data did not cover the whole size range at that time.

centrations of recombination products and all neutral clusters are depicted for new particle formation event and non-event days. Figure 5 also shows that the concentration of recombination products was on average slightly higher on new particle formation event days than on non-event days, except for the afternoon hours.

The obtained results are in reasonable agreement with the results of earlier studies, in which the concentration of recombination products has been calculated from Eq. (6) not including the condensational growth term. Recently, Kulmala et al. (2013) concluded that on average only a minor

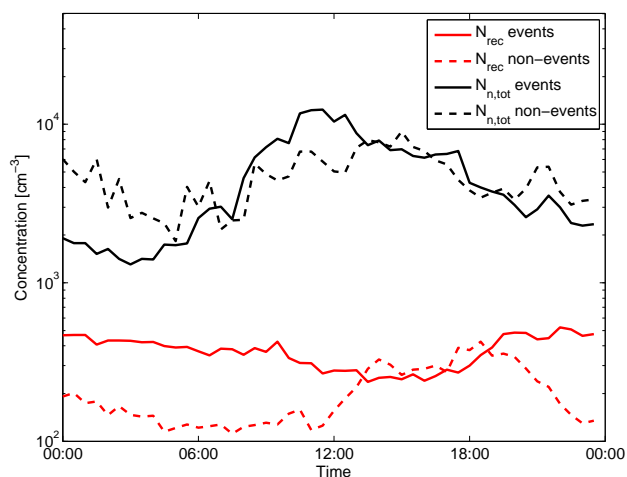


Fig. 5. The median diurnal variations of the concentrations of recombination products (N_{rec}) and all neutral clusters ($N_{\text{n,tot}}$) in the size range of 0.9–2.1 nm on new particle formation event and non-event days.

fraction of sub-2 nm neutral clusters observed in Hyytiälä originates from ion–ion recombination. By measuring the concentrations of sub-3 nm particles at the same site, Lehtipalo et al. (2009) observed that the fraction of recombination products of all neutral clusters is on average low ($\sim 5\%$) but varies a lot from day to day. Furthermore, the comparison between the formation rates of neutral clusters due to ion–ion recombination and the total particle formation rates indicates that ion–ion recombination has only minor contribution to particle formation in boreal forest (Kulmala et al., 2007; Manninen et al., 2009a). However, the model simulations by Yu and Turco (2008) suggest much greater significance for recombination than the studies based on field measurements. This discrepancy illustrates the fact that the details of the dynamics of sub-3 nm charged and neutral clusters are still not well known. This makes both the modeling and the theoretical calculations of the ion–ion recombination process challenging. In addition, the uncertainties in measuring the size distributions of neutral and charged clusters in this size range are also relatively large. For more discussion about the role of ion-mediated processes in atmospheric new particle formation, see Hirsikko et al. (2011).

3.2 Sensitivity of the method to uncertainties of the condensational growth effect

In Sect. 2.2.1 we noted that we can calculate the concentration of recombination products from Eq. (5) only if we know the growth rates of clusters in each size class. Otherwise, we need to neglect the effect of condensational growth and calculate the recombination product concentration from Eq. (6). In this study, we solved this problem by using the average growth rates for new particle formation periods presented by

Kulmala et al. (2013). However, in reality, these growth rates may not be representative regarding the whole measurement period, which also includes time periods with no new particle formation. Thus, in this section we aim to assess how sensitive the obtained results are to uncertainties in the growth rates. Furthermore, we examine how the results change if we assume that the condensational growth term is negligible and calculate the concentration of recombination products from Eq. (6) as has been done in earlier studies (Lehtipalo et al., 2009; Kulmala et al., 2013).

To evaluate the sensitivity of our results to the changes in the growth rates, we examined how the results change if the growth rate increases with the increasing cluster size more slowly than shown in the data by Kulmala et al. (2013). The growth rates assumed for different size classes in this analysis are presented in Table 1, and the fractions of recombination products of all neutral clusters obtained with these growth rates are illustrated in Fig. 6a. We can see that the distribution of the fraction of recombination products looks very similar to the distribution obtained with the more strongly increasing growth rate shown by Fig. 3. The only difference is that with the more gradually increasing growth rate the fraction of recombination products reached slightly higher values. The highest median fraction obtained in the size classes between 1.5 and 1.9 nm was 17%. Thus, it seems that also in the conditions where the cluster growth accelerates more slowly than is typical during new particle formation events, most of the neutral clusters observed in Hyytiälä originate from other processes than ion–ion recombination.

To examine how the results change if the effect of condensational growth is neglected, we also calculated the concentration of recombination products in different size classes from Eq. (6). However, in this case we noticed that it is not reasonable to assume that the coefficient λ , describing the fraction of stable recombination products, equals unity because the concentrations of recombination products obtained with $\lambda = 1$ were often larger than the total neutral cluster concentrations. Thus, we determined the maximum value for the coefficient, λ_{max} , by using the method presented by Kulmala et al. (2013). For the smallest size class (0.9–1.1 nm) λ_{max} was equal to 1 as we could not find the upper limit for the coefficient by using this method. Also, in the next size class (1.1–1.3 nm), the value of λ_{max} was relatively high (0.63). However, in the size classes between 1.3 and 2.1 nm the maximum fraction of stable recombination products varied between 0.15 and 0.37. Finally, we calculated the concentration of recombination products in different size classes from Eq. (6) by replacing λ with λ_{max} . Figure 6b depicts the fraction of recombination products of all neutral clusters obtained for different size classes with this method. The fraction of recombination products appeared to have its maximum at smaller sizes than when the effect of condensational growth was taken into account (Fig. 3). The median values of the fraction were also clearly lower, varying between 0.3 and 5%. This is mainly due to the fact that in this analysis the

coefficient λ was not assumed to equal 1, as was done when the condensational growth term was included in the calculations. In fact, it seems that if the effect of condensational growth is neglected but the value of the coefficient λ is still assumed to equal 1, as was the case for example in Lehtipalo et al. (2009), the concentration of recombination products is probably overestimated.

4 Summary and conclusions

In this paper, we presented and evaluated a method for determining the size distribution of recombination products from the measured size distributions of charged and neutral clusters. This method takes into account the production of recombination products in the collisions between oppositely charged ions and the loss of them by coagulation. In addition, contrary to earlier studies, the loss and gain of recombination products due to condensational growth are also considered. We applied our method to the size distribution data measured in Hyytiälä, Finland, during spring 2011. From that data we determined the production rate of neutral clusters by ion–ion recombination and the concentration of recombination products in six equally spaced size classes between 0.9 and 2.1 nm. In addition, the proportion of recombination products of all neutral clusters was investigated.

The recombination production rate was highest in the size classes between 1.3 and 1.7 nm and lowest in the smallest (0.9–1.1 nm) and the largest (1.9–2.1 nm) size classes. The median recombination production rates varied between $7 \times 10^{-3} \text{ cm}^{-3} \text{ s}^{-1}$ and $7 \times 10^{-2} \text{ cm}^{-3} \text{ s}^{-1}$ in different size classes. The concentration of recombination products had a maximum in the size classes between 1.5 and 1.9 nm in which the median concentration was 69 cm^{-3} . The concentration was lowest in the smallest size class (0.9–1.1 nm) with the median value of 6 cm^{-3} .

On average, recombination products accounted only for 1.5 % of all neutral clusters in the size range of 0.9–2.1 nm during the measurement period. However, the fraction of recombination products of all neutral clusters varied depending on the examined size class. The median fraction of recombination products was lowest, 0.2 %, in the smallest size class (0.9–1.1 nm), and highest, 13 %, in the size classes between 1.5 and 1.9 nm. The temporal variation of the fraction was also strong. The results are in agreement with earlier studies where a minor contribution of recombination products to the neutral cluster population was observed using particle size distribution data from Hyytiälä (Lehtipalo et al., 2009; Kulmala et al., 2013). Still, it has to be noted that in those studies the effect of condensational growth on the recombination product size distribution has been neglected. In this study, however, we included the condensational growth effect in our calculations by estimating the cluster growth rates from the data presented by Kulmala et al. (2013).

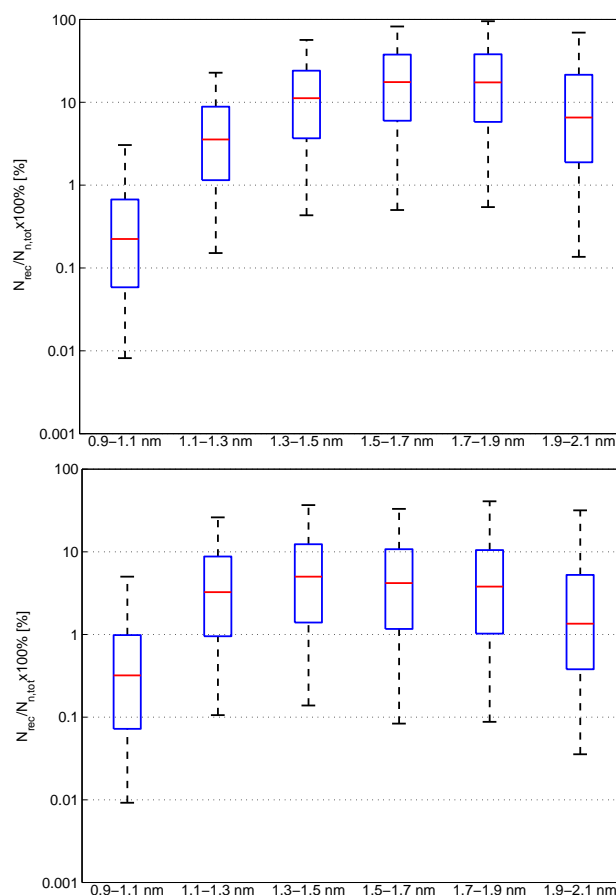


Fig. 6. The percentage of recombination products of all neutral clusters in different size classes (top) when assuming that the cluster growth rate increases more slowly with the increasing size than shown by experimental data (bottom) when the effect of condensational growth is neglected and the coefficient λ is not assumed to equal 1. The red lines show the medians, the blue boxes indicate the 25th and 75th percentiles, and the vertical bars show the 5th and 95th percentiles.

To evaluate the sensitivity of our results to uncertainties in the growth rates, we examined how the results change if the growth rate increases more gradually with the increasing cluster size than shown by the data that we used. We concluded that although the fractions of recombination products of all neutral clusters were slightly higher when using more slowly increasing growth rate, the results did not change significantly. We also examined how the fraction of recombination products of all neutral clusters changes if the effect of condensational growth is assumed to be negligible. It seems that in this case we can no longer neglect the fragmentation of newly formed recombination products because by doing so we end up overestimating the concentration of recombination products. Therefore, we used the method presented by Kulmala et al. (2013) to estimate the maximum fraction of stable recombination products. By using this method we

obtained lower values for the fraction of recombination products of all neutral clusters than when the effect of condensational growth was taken into account.

Overall, our method can be assumed to provide a reasonable maximum estimate of the contribution of recombination products to atmospheric cluster concentrations. In the light of our results, it seems that the effect of condensational growth on the size distribution of recombination products should not be neglected, provided that the values for the cluster growth rates are known. Thus, determining the size distribution of recombination products more accurately in the future would require more precise measurements of the size distributions of atmospheric clusters. In addition, the dependency of the recombination coefficient on environmental conditions, especially on temperature, and on the masses of colliding ions should be understood better so that it could be included in the calculations. Finally, more knowledge of the fragmentation of recombination products would be needed to establish how important ion–ion recombination truly is for the dynamics of atmospheric clusters.

Acknowledgements. The financial support from a European Research Council (ERC) Advanced Grant (ATM-NUCLE, 227463), the Academy of Finland Centre of Excellence program (project no. 1118615), and the Nordic Top-level Research Initiative (TRI) Cryosphere-Atmosphere Interactions in a Changing Arctic Climate (CRAICC) is gratefully acknowledged.

Edited by: S. M. Noe

References

- Aalto, P. P., Hämeri, K., Becker, E., Weber, R., Salm, J., Mäkelä, J. M., Hoell, C., O'Dowd, C. D., Karlsson, H., Hansson, H., Väkevä, M., Koponen, I., Buzorius, G., and Kulmala, M.: Physical characterization of aerosol particles during nucleation events, *Tellus B*, 53, 344–358, 2001.
- Bates, D. R.: Ion–ion recombination in an ambient gas, *Adv. Atomic Molecular Phys.*, 20, 1–40, 1985.
- Biondi, M.: Atmospheric electron-ion and ion-ion recombination processes, *Can. J. Chem.*, 47, 1711–1719, 1968.
- Böhringer, H., Fahey, D. W., Lindinger, W., Howorka, F., Fehsenfeld, F. C., and Albritton, D. L.: Mobilities of several mass-identified positive and negative ions in air, *Int. J. Mass Spectrom. Ion Proc.*, 81, 45–65, 1987.
- Ehn, M., Junninen, H., Schobesberger, S., Manninen, H. E., Franchin, A., Sipilä, M., Petäjä, T., Kerminen, V.-M., Tammet, H., Mirme, A., Mirme, S., Hörrak, U., Kulmala, M., and Worsnop, D. R.: An instrumental comparison of mobility and mass measurements of atmospheric small ions, *Aerosol Sci. Technol.*, 45, 4, 522–532, 2011.
- Hari, P. and Kulmala, M.: Station for Measuring Ecosystem–Atmosphere Relations (SMEAR II), *Boreal Environ. Res.*, 10, 315–322, 2005.
- Hirsikko, A., Nieminen, T., Gagné, S., Lehtipalo, K., Manninen, H. E., Ehn, M., Hörrak, U., Kerminen, V.-M., Laakso, L., McMurry, P. H., Mirme, A., Mirme, S., Petäjä, T., Tammet, H., Vakkari, V., Vana, M., and Kulmala, M.: Atmospheric ions and nucleation: a review of observations, *Atmos. Chem. Phys.*, 11, 767–798, doi:10.5194/acp-11-767-2011, 2011.
- Hoppel, W. A. and Frick, G. M.: Ion-aerosol attachment coefficients and the steady-state charge distribution on aerosols in a bipolar ion environment, *Aerosol Sci. Technol.*, 5, 1–21, 1986.
- Kazil, J., Stier, P., Zhang, K., Quaas, J., Kinne, S., O'Donnell, D., Rast, S., Esch, M., Ferrachat, S., Lohmann, U., and Feichter, J.: Aerosol nucleation and its role for clouds and Earth's radiative forcing in the aerosol-climate model ECHAM5-HAM, *Atmos. Chem. Phys.*, 10, 10733–10752, doi:10.5194/acp-10-10733-2010, 2010.
- Kerminen, V.-M., Paramonov, M., Anttila, T., Riipinen, I., Fountoukis, C., Korhonen, H., Asmi, E., Laakso, L., Lihavainen, H., Swietlicki, E., Svenningsson, B., Asmi, A., Pandis, S. N., Kulmala, M., and Petäjä, T.: Cloud condensation nuclei production associated with atmospheric nucleation: a synthesis based on existing literature and new results, *Atmos. Chem. Phys.*, 12, 12037–12059, doi:10.5194/acp-12-12037-2012, 2012.
- Kilpatrick, W. D.: An experimental mass-mobility relation for ions in air at atmospheric pressure, *Proc. 19th Annu. Conf. Mass. Spectrosc.*, 2–7 May 1971, Atlanta, 320–325, 1971.
- Kulmala, M., Dal Maso, M., Mäkelä, J. M., Pirjola, L., Väkevä, M., Aalto, P., Miiikkulainen, P., Hämeri, K., and O'Dowd, C. D.: On the formation, growth and composition of nucleation mode particles, *Tellus*, 53B, 479–490, 2001.
- Kulmala, M., Riipinen, I., Sipilä, M., Manninen, H., Petäjä, T., Junninen, H., Dal Maso, M., Mordas, G., Mirme, A., Vana, M., Hirsikko, A., Laakso, L., Harrison, R. M., Hanson, I., Leung, C., Lehtinen, K. E. J., and Kerminen, V.-M.: Towards direct measurement of atmospheric nucleation, *Science*, 318, 89–92, 2007.
- Kulmala, M., Kontkanen, J., Junninen, H., Lehtipalo, K., Manninen, H. E., Nieminen, T., Petäjä, T., Sipilä, M., Schobesberger, S., Rantala, P., Franchin, A., Jokinen, T., Järvinen, E., Äijälä, M., Kangasluoma, J., Hakala, J., Aalto, P., Paasonen, P., Mikkilä, J., Vanhanen, J., Aalto, J., Hakola, H., Makkonen, U., Ruuskanen, T., Mauldin III, R. L., Duplissy, J., Vehkamäki, H., Bäck, J., Kortelainen, A., Riipinen, I., Kurten, T., Johnston, M. V., Smith, J. N., Ehn, M., Mentel, T. F., Lehtinen, K. E. J., Laaksonen, A., Kerminen, V.-M., and Worsnop, D. R.: Direct observations of atmospheric aerosol nucleation, *Science*, 339, 943–946, 2013.
- Lehtipalo, K., Sipilä, M., Riipinen, I., Nieminen, T., and Kulmala, M.: Analysis of atmospheric neutral and charged molecular clusters in boreal forest using pulse-height CPC, *Atmos. Chem. Phys.*, 9, 4177–4184, doi:10.5194/acp-9-4177-2009, 2009.
- Mäkelä, J. M., Jokinen, V., Mattila, T., Ukkonen, A., and Keskinen, J.: Mobility distribution of acetone cluster ions, *J. Aerosol Sci.*, 27, 175–190, 1996.
- Makkonen, R., Asmi, A., Kerminen, V.-M., Boy, M., Arneth, A., Hari, P., and Kulmala, M.: Air pollution control and decreasing new particle formation lead to strong climate warming, *Atmos. Chem. Phys.*, 12, 1515–1524, doi:10.5194/acp-12-1515-2012, 2012.
- Manninen, H. E., Nieminen, T., Riipinen, I., Yli-Juuti, T., Gagné, S., Asmi, E., Aalto, P. P., Petäjä, T., Kerminen, V.-M., and Kulmala, M.: Charged and total particle formation and growth rates during EUCAARI 2007 campaign in Hyytiälä, *Atmos. Chem. Phys.*, 9, 4077–4089, doi:10.5194/acp-9-4077-2009, 2009a.

- Manninen, H. E., Petäjä, T., Asmi, E., Riipinen, I., Nieminen, T., Mikkilä, J., Hörrak, U., Mirme, A., Mirme, S., Laakso, L., Kerminen, V.-M., and Kulmala, M.: Long-term field measurements of charged and neutral clusters using Neutral cluster and Air Ion Spectrometer (NAIS), *Boreal Environ. Res.*, 14, 591–605, 2009b.
- McGowan, S.: Ion–ion recombination in laboratory air, *Phys. Med. Biol.*, 10, 25–40, 1965.
- Merikanto, J., Spracklen, D. V., Mann, G. W., Pickering, S. J., and Carslaw, K. S.: Impact of nucleation on global CCN, *Atmos. Chem. Phys.*, 9, 8601–8616, doi:10.5194/acp-9-8601-2009, 2009.
- Mirme, S. and Mirme, A.: The mathematical principles and design of the NAIS – a spectrometer for the measurement of cluster ion and nanometer aerosol size distributions, *Atmos. Meas. Tech.*, 6, 1061–1071, doi:10.5194/amt-6-1061-2013, 2013.
- Nolan, P. J.: The recombination law for weak ionization, *Nature*, 148, 26–26, 1941.
- Raes, F., Van Dingenen, R., Vignati, E., Wilson, J., Putaud, J. P., Seinfeld, J. H., and Adams, P.: Formation and cycling of aerosols in the global troposphere, *Atmos. Environ.*, 34, 4215–4240, 2000.
- Sorokin, A. and Mirabel, P.: Ion recombination in aircraft exhaust plumes, *Geophys. Res. Lett.*, 28, 955–958, 2001.
- Spracklen, D. V., Carslaw, K. S., Kulmala, M., Kerminen, V.-M., Mann, G. W., and Sihto, S.-L.: The contribution of boundary layer nucleation events to total particle concentrations on regional and global scales, *Atmos. Chem. Phys.*, 6, 5631–5648, doi:10.5194/acp-6-5631-2006, 2006.
- Swider, W.: Ionic mobility, mean mass, and conductivity in the middle atmosphere from near ground level to 70 km, *Radio Science*, 23, 389–399, 1988.
- Tammet, H.: Size and mobility of nanometer particles, clusters and ions, *J. Aerosol Sci.*, 26, 459–475, 1995.
- Tammet, H. and Kulmala, M.: Simulation tool for atmospheric aerosol nucleation bursts, *J. Aerosol Sci.*, 36, 173–196, 2005.
- Tammet, H., Hörrak, U., Laakso, L., and Kulmala, M.: Factors of air ion balance in a coniferous forest according to measurements in Hyytiälä, Finland, *Atmos. Chem. Phys.*, 6, 3377–3390, doi:10.5194/acp-6-3377-2006, 2006.
- Turco, R. P., Hao, J.-X., and Yu, F.: A new source of tropospheric aerosols: Ion–ion recombination, *Geophys. Res. Lett.*, 25, 635–638, 1998.
- Wang, M. and Penner, J. E.: Aerosol indirect forcing in a global model with particle nucleation, *Atmos. Chem. Phys.*, 9, 239–260, doi:10.5194/acp-9-239-2009, 2009.
- Vanhanen, J., Mikkilä, J., Lehtipalo, K., Sipilä, M., Manninen, H. E., Siivola, E., Petäjä, T., and Kulmala, M.: Particle size magnifier for nano-CN detection, *Aerosol Sci. Tech.*, 45, 533–542, 2011.
- Yu, F. and Turco, R.: Case studies of particle formation events observed in boreal forests: implications for nucleation mechanisms, *Atmos. Chem. Phys.*, 8, 6085–6102, doi:10.5194/acp-8-6085-2008, 2008.
- Yu, F., Luo, G., Bates, T. S., Anderson, B., Clarke, A., Kapustin, V., Yantosca, R. M., Wang, Y., and Wu, S.: Spatial distributions of particle number concentrations in the global troposphere: Simulations, observations, and implications for nucleation mechanisms, *J. Geophys. Res.*, 115, D17205, doi:10.1029/2009JD013473, 2010.
- Zhang, R., Khalizov, A., Wang, L., Hu, M., and Xu, W.: Nucleation and growth of nanoparticles in the atmosphere, *Chem. Rev.*, 112, 1957–2011, 2012.